metals

MDPI

Article

Effects of Process Control Agent Amount, Milling Time, and Annealing Heat Treatment on the Microstructure of AlCrCuFeNi High-Entropy Alloy Synthesized through Mechanical Alloying

Negar Yazdani [1], Mohammad Reza Toroghinejad [1], Ali Shabani [1] and Pasquale Cavaliere [2,*]

[1] Department of Materials Engineering, Isfahan University of Technology, Isfahan 84156-83111, Iran; n.yazdani@ma.iut.ac.ir (N.Y.); toroghi@iut.ac.ir (M.R.T.); ali.shabani@ma.iut.ac.ir (A.S.)
[2] Department of Innovation Engineering, University of Salento, Via per Arnesano, 73100 Lecce, Italy
* Correspondence: pasquale.cavaliere@unisalento.it

Abstract: This study was conducted to investigate the characteristics of the AlCrCuFeNi high-entropy alloy (HEA) synthesized through mechanical alloying (MA). In addition, effects of Process Control Agent (PCA) amount and milling time were investigated using X-ray diffraction analysis (XRD), scanning electron microscopy (SEM), and energy dispersive X-ray spectroscopy (EDS). The results indicated that the synthesized AlCrCuFeNi alloy is a dual phase (FCC + BCC) HEA and the formation of the phases is strongly affected by the PCA amount. A high amount of PCA postponed the alloying process and prevented solid solution formation. Furthermore, with an increase in the PCA amount, lattice strain decreased, crystallite size increased, and the morphology of the mechanically alloyed particles changed from spherical to a plate-like shape. Additionally, investigation of thermal properties and annealing behavior at different temperatures revealed no phase transformation up to 400 °C; however, the amount of the phases changed. By increasing the temperature to 600 °C, a sigma phase (σ) and a B2-ordered solid solution formed; moreover, at 800 °C, the FCC phase decomposed into two different FCC phases.

Keywords: high-entropy alloy; Process Control Agent; annealing; XRD; microstructure

Citation: Yazdani, N.; Toroghinejad, M.R.; Shabani, A.; Cavaliere, P. Effects of Process Control Agent Amount, Milling Time, and Annealing Heat Treatment on the Microstructure of AlCrCuFeNi High-Entropy Alloy Synthesized through Mechanical Alloying. *Metals* **2021**, *11*, 1493. https://doi.org/10.3390/met11091493

Academic Editor: Chunfeng Hu

Received: 24 August 2021
Accepted: 17 September 2021
Published: 20 September 2021

1. Introduction

With the advancement of technology, the need for materials that are superior and unique in terms of various aspects such as availability, economic efficiency, and properties, has led to the discovery of advanced materials. The unique design of high entropy alloys (HEAs) has made these alloys one of the most advanced alloys and a new step in improving the performance of materials in the industry. HEAs have been defined as solid solution alloys with five or more principal elements, with an atomic concentration range of 5–35% [1–3]. As the name of these alloys indicates, high entropy of mixing has a key role in their properties, decreases the Gibbs free energy, facilities the formation of simple crystalline structures including FCC, BCC, or FCC + BCC, and restricts the formation of complex structures such as intermetallic compounds [4,5]. In addition to the entropy of mixing (ΔS_{mix}), parameters such as enthalpy of mixing (ΔH_{mix}), and atomic size difference (δ) were also reported as parameters effective on the formation of solid solution phases in HEAs [2,6].

There are a variety of processing routes for the synthesis of HEAs, which can be categorized into four different classes of routes including fabrication from (1) liquid state, (2) solid-state, (3) and gas state, and (4) fabrication through electrochemical process [2,7]. Mechanical alloying (MA) is well-known as a solid-state and non-equilibrium fabrication method that can facilitate the formation of a metastable phase and was widely used for the fabrication of nanocrystalline materials and HEAs [8–11]. Recently, Varalakshmi et al. [12]

used MA method to produce nanostructured equiatomic high entropy solid solutions from binary to hexanary compositions in AlFeTiCrZnCu system with a simple BCC crystalline structure. Fabrication of nanocrystalline HEAs with simple FCC, BCC, and/or FCC + BCC crystalline structures through MA process has been reported in many different HEA systems such as AlCuNiFeCr [13], AlCoCrFeNi [9], CoCrCuFeNi [14], AlCoCrCuFe [7], and AlCoCrCuFeNi [15].

Generally, MA process involves cold welding between particles, plastic deformation, and fracture of particles. These two processes reduce the diffusion distance through contact with the clean surfaces of the powder particles. Fracture reduces the particle size, and as a result, increases the contact surface area between particles; moreover, cold welding leads to bonding between particles, and consequently, inter-diffusion [16–19]. However, in alloying systems with a high percentage of a soft and flexible material, the balance between cold welding and fracture is disrupted and cold welding acts as the dominant mechanism [16]. To overcome this problem, a Process Control Agent (PCA) is usually used and the lubricant effect of PCA prevents excessive cold welding of the powders [16,20,21]. It should be noted that the presence of these compounds can cause microstructural changes in the alloying system [16,21,22]. Lu and Zhang [23] revealed that a small amount of PCA might lead to fast inter-diffusion and reaction between Al and Mg during MA process. Nouri et al. [21] asserted that increasing PCA content leads to a remarkable increase in Vickers hardness of the sintered titanium alloy. Additionally, Duan et al. [22] claimed that increased amount of PCA plays an active role in the crystallinity of powders, and regulates the thickness and size distribution of flake particles in $FeCoNiAlCr_{0.9}$ HEA.

It has been reported that annealing treatments directly influence different properties of HEAs; however, thermal stability has also been reported in these alloys [13,14,24,25]. Thangaraju et al. [14] showed that single FCC phase CoCrCuFeNi HEA has a thermal stability of up to 800 °C. Nevertheless, with a further increase in temperature the FCC phase decomposed into two different FCC phases due to the positive enthalpy of mixing between Cu and other elements. Shabani et al. [24] reported that the FeCrCuMnNi HEA has a thermal stability of up to 600 °C and the formation of a σ phase led to a sharp drop in the mechanical properties.

Recently, using the MA method, Yurkova et al. [13] fabricated AlCrCuFeNi HEA consisting of a single BCC phase. They also studied different properties of the alloy; however, more investigation in some aspects seems necessary. Therefore, the aim of this research was to investigate the effect of PCA amount on structural properties and microstructure of the AlCrCuFeNi HEA and perform an in-depth investigation of the thermal behavior of the alloy.

2. Material and Methods

The elemental powders of Al, Cr, Cu, Fe, and Ni, with more than 99% purity (Merck Co., Gernsheim, Germany) and particle size of less than 45 μm, were used as raw materials. The physical characteristics of the constituent elements of the alloy can be found elsewhere [26]. In addition, to ensure the purity of the powders, an energy-dispersive X-ray spectroscope (EDS; ALS2300C; SERON, Uiwang, Korea) was used. Subsequently, equal atomic proportions of the powders were mixed and milled for 60 h using a planetary ball mill (QM-3SP4; Nanda Co., Ltd., Seoul, Korea) in a steel vial. Milling was conducted at a rotation speed of 350 rpm and under Argon atmosphere to prevent oxidation. In order to investigate the effects of PCA amount on the characteristics of the milled powders, 4 different amounts of stearic acid (1, 2, 3, and 4 wt. % of the total amount of powder) were used as PCA. Hardened chromium steel balls were used for milling with a ball-to-powder weight ratio of 10:1. Every 10 h, a small amount of powder was taken from the mixture, placed inside the vacuum glove box, and sent for X-ray diffraction analysis (XRD; Cu-Kα radiation 1.542 °A) and scanning electron microscopy (SEM; XL30, Philips, Amsterdam, The Netherlands) to investigate the phase evolution and morphology of the powders. EDS was also used after milling to study the chemical composition of the samples, and elemental

distribution and homogeneity of the powders. Differential Scanning Calorimetry (DSC; L81, Linseis, Selb, Germany) was performed on the powder samples milled for 60 h, with 2 wt. % PCA, heated from ambient temperature to 1200 °C, at a rate of 10 °C/min, and under Argon atmosphere. This analysis was carried out to verify the thermal stability of the alloy. The procedure was followed by annealing of the 60-h-milled powder samples with 2% PCA; the temperature of annealing was 400, 600, 800, and 1000 °C, chosen based on the results of the DSC analysis. The heating rate was 10 °C/min and samples were maintained at each temperature for 1 h under Argon atmosphere. After heat treatment, each sample was analyzed using XRD in order to monitor the changes in the crystalline structure of the powder samples.

3. Results and Discussion

3.1. Thermodynamics of the Alloy

To date, some theoretical criteria have been introduced to predict phase formation in HEAs such as enthalpy of mixing (ΔH_{mix}), entropy of mixing (ΔS_{mix}), atomic size difference (δ), and the Valence electron concentration (VEC) [6,27]. The calculated values of these parameters with their criteria for formation of HEA solid solution are presented in Table 1. As shown, all parameters are well within the range needed for the formation of HEA solid solution. Therefore, according to the measured data the formation of a dual-phase HEA (FCC + BCC) with a simple solid solution structure in the AlCrCuFeNi alloying system is expected during MA process.

Table 1. The general theoretical criterion required for the formation of solid solution HEA and those calculated for AlCrCuFeNi HEA.

Item	Mixing Enthalpy (ΔH_{mix}, kJ/mol)	Mixing Entropy (ΔS_{mix}, J/k.mol)	Radius Difference	Valence Electron Concentration (VEC)
Criterions	$-10 < \Delta H < +5$	$\geq$13.38	$\delta < 6.6\%$	$6.87 \leq VEC < 8$ for FCC + BCC
Calculated for AlCrCuFeNi	−4	13.38	5.62%	7.6

3.2. Effect of Process Control Agent Amount

In order to investigate the effect of PCA amount on the properties of the produced AlCrCuFeNi alloy, different amounts of PCA (1, 2, 3, and 4 wt. % of the total powder weigh) were added to the powder mixture during MA process. After 60 h of milling, XRD analysis was conducted on each sample to evaluate the effect of PCA. Figure 1 shows the XRD patterns of AlCrCuFeNi HEA powder with various PCA amounts after 60 h of milling. It can be seen that with decrease in PCA amounts, elements' peaks almost disappear from the XRD patterns of all samples, and as expected, a dual-phase HEA forms after 60 h of milling in the presence of 2 wt. % of PCA. The dual-phase structure was also achieved in the presence of 1 wt. % of PCA. Generally, cold welding, fracture, and inter-diffusion are the controlling parameters during MA and strongly affect the alloying process [16,18]. Cold welding and fracturing cause the clean surfaces of the powder particles to be always in contact with each other, and therefore, minimize the diffusion distance for elements [16,19]. Using high amounts of PCA in the MA process leads to the formation of a PCA cover on the surface of particles; this cover acts as a lubricant between particles and between particles and balls. This lubricant effect of PCA strongly reduces the rate of cold welding and fracture processes during MA and consequently, postpones the alloying process; this was seen in the XRD results as the peaks of elements remaining sharp in the presence of 3 and 4 wt. % of PCA. Additionally, the presence of a PCA layer on the surface of particles leads to the increment of inter-diffusion distance between particles, which reduces the ideal mixture of elements for solid solution formation and postpones the alloying process.

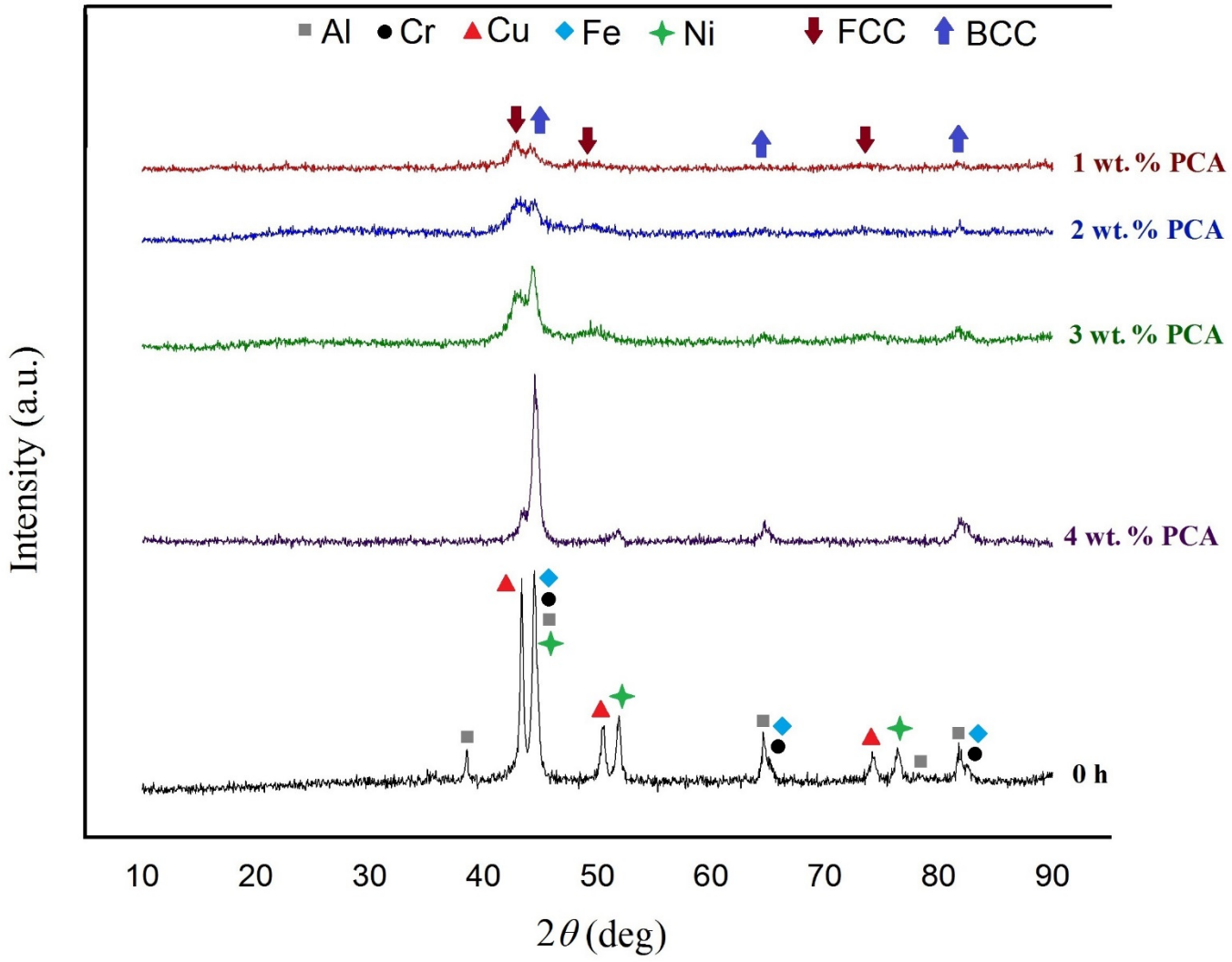

Figure 1. XRD patterns of AlCrCuFeNi alloy after 60 h of milling with different amounts of Process Control Agent—PCA (1, 2, 3, and 4 wt. %).

Effects of PCA amount on the average crystallite size and lattice strain of the AlCrCuFeNi alloy were calculated using Scherer and Williamson-Hall equations based on the XRD results [28,29] and are presented in Figure 2. It is evident that with increase in PCA amount, crystallite size increases and lattice strain decreases. The maximum lattice strain (0.97%) and the minimum crystallite size (7 nm) are seen in the sample with the least amount of PCA (1 wt. %), and conversely, the minimum lattice strain (0.25%) and the maximum crystallite size (20 nm) are seen in the sample with the highest amount of PCA (4 wt. %). As explained, increase in PCA amount could affect the mechanically alloyed powder in two ways, first, cold welding between the surfaces of particles decreases due to the lubricant effect of PCA, and second, inter-diffusion between particles reduces due to the formation of a PCA layer on the surface of particles and increment of inter-diffusion distance between particles [20,23]. With increase in PCA amount, a decrease in inter-diffusion between particles occurs, which leads to decreased atomic size mismatch between constituent elements, and consequently, decreased lattice strain. In addition, formation of a lubricant layer on the surfaces and decrease in cold welding lead to lower severe plastic deformation of the particles, which results in decrease a in grain boundary fraction and structural defects, such as dislocations, vacancies, etc., in the crystal structure; therefore, lattice strain decreases [20,30,31]. Moreover, it is well-known that, during severe plastic deformation, increase in dislocation density and their rearrangement in the form of

low-angle grain boundaries leads to the formation of smaller diffraction domains; therefore, increase in PCA amount results in lower dislocation density, and consequently, lower crystallite size [20,30]. Shaw et al. [20] claimed that with increase in PCA amount, plastic deformation followed by crystalline defects is reduced due to the lubricating effect of the PCA in $Al_{93}Fe_3Ti_2Cr_2$ HEA. During milling, PCA acts as a lubricant and reduces the coefficient of friction of the powder particles with each other, with the mill chamber wall, and with the balls. Therefore, due to the easy slipping of the particles on each other or on balls, the rate of plastic deformation decreases [32].

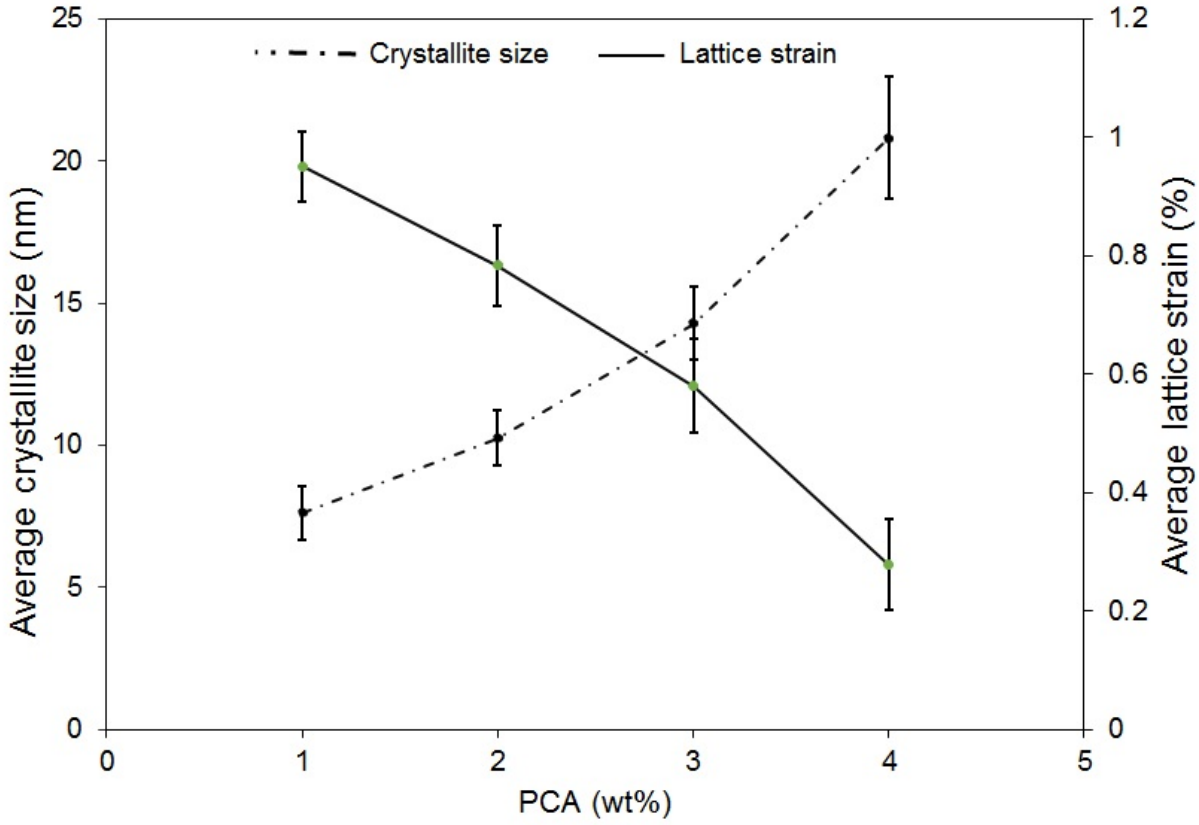

Figure 2. Variation in average crystallite size (nm) and lattice strain (%) of mechanically alloyed AlCrCuFeNi HEA after 60 h of milling as a function of PCA amount.

Figure 3 illustrates the SEM images of the powders synthesized in the presence of different amounts of PCA with different magnifications. As revealed in this figure, with increase in PCA amount, particle size decreases, and the shape distribution of particles becomes non-uniform and more plate-like particles are seen. The average particle size of the powders was measured and the particle sizes were in the ranges of 28–65, 8–44, 4–26, and 1–11 μm in the samples with 1, 2, 3, and 4 wt. % of PCA, respectively; this confirms the descending trend of average particle size. As previously explained, PCA has a lubricant effect and prevents excessive cold welding of the powders; therefore, particle size decreases with increase in PCA amount.

During milling, the morphology of particles with a soft matrix changes to a plate-like morphology, and then, with increase in deformation and occurrence of work hardening and brittleness, these plate-like particles break into smaller particles [16,18,33]. However, increment of PCA amount leads to lower deformation and work hardening in particles due to the lubricant effect of PCA. This results in the formation of a larger number of plate-like particles, which leads to a non-uniform distribution shapes of particles.

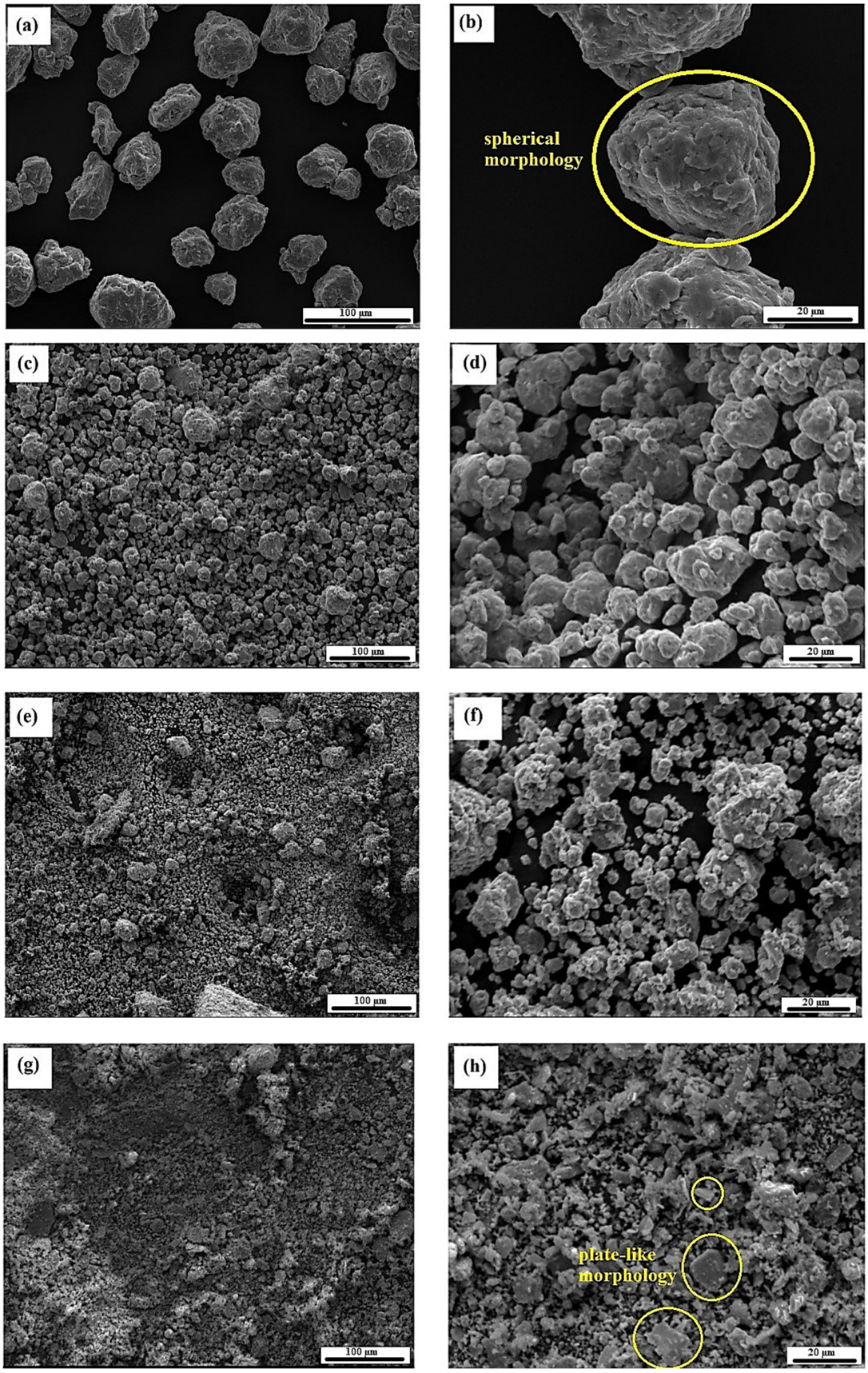

Figure 3. SEM images of mechanically alloyed AlCrCuFeNi HEA after 60 h of milling in the presence of (**a**,**b**) 1, (**c**,**d**) 2, (**e**,**f**) 3, and (**g**,**h**) 4 wt. % of PCA amount.

On the one hand, increase in PCA amount to 3 or 4 wt. % delayed the alloying process, and therefore, additional time might be required for the fulfillment of the MA process and solid solution formation. On the other hand, in the presence of a low amount of PCA (1 wt. %), a balance is not reached between fracture and cold welding, which leads to increased particle size. Therefore, the 2 wt. % of PCA seems to be the optimum amount in this alloying system and was chosen for the MA process.

3.3. Synthesis of AlCrCuFeNi Alloy with 2 wt. % of Process Control Agent

Based on the results presented in the previous section, 2 wt. % of PCA was used for the fabrication of AlCrCuFeNi HEA at different MA process times (maximum: 60 h). Samples were examined after different time periods and the XRD patterns are shown in Figure 4. As shown in this figure, the initial mixture contains peaks associated with Al, Cr, Cu, Fe, and Ni, which are the initial elements. Subsequently, due to repeated collision and cold welding of the particles, which causes the diffusion of the elements into each other's lattice, peak intensities decrease; therefore, the peaks of Al, Cu, and Ni tend to disappear after 20 h of milling. It is known that elements with lower melting point (Al, Cu, and Ni here), which actually means less bonding energy, tend to have higher diffusion rates [26], and their diffusion leads to the formation of solid solutions. BCC and FCC phase form in the alloy after 30 h of milling and after 40 h of milling, respectively. By milling up to 60 h, the intensity of peaks associated with FCC rises, and those associated with BCC decreases. Yurkova et al. [13] however reported a faster formation of solid solutions (after almost 5 h) in the same alloying system, which is directly related to the higher rotation speed used. With increase in rotation speed, the amount of energy transferred to the powder particles, and thus, the diffusion of the atoms of the elements increases; therefore, the formation of a solid solution occurs sooner [28].

Lattice parameters of the FCC and BCC phases, after 60 h of milling, were measured at 0.36415 and 0.28853 nm, respectively. The lattice parameter of FCC is close to that of Cu; thus, the increase in the FCC phase amount can be attributed to the segregation of Cu from the system due to the high positive mixing enthalpy (ΔH_{mix}) of Cu with other elements [14,34]. Moreover, the lattice parameter of BCC is close to that of Fe and Cr; however, Cr has a higher melting point than Fe and is less active in the diffusion. Therefore, Cr acts as the solvent for the formation of BCC solid solution [26].

In addition, Figure 4 also shows that no intermetallic compound formed in this alloying system during the MA process, which is attributed to two factors. The first is the high entropy of the system that inhibits the formation of intermetallic phases with low amount of entropy of mixing [4,30]. The second is the severe strain induced in the powder particles that increases the stored energy of the system through enhancement of the volume of grain boundaries and increasing of crystal defects such as dislocation and vacancies. The higher amount of stored energy acts as a driving force for solid solution formation [26,30].

The variations in crystallite size and lattice strain of the AlCrCuFeNi HEA as a function of milling time are presented in Figure 5. It can be seen that with increase in the milling time, the average crystallite size continually decreases, while the average lattice strain increases. As mentioned earlier, an increase in lattice strain is attributed to the severe plastic deformation of the particles during milling. This significantly increases structural defects such as dislocations and vacancies, thus leading to a higher lattice strain [30]. However, rearrangement of dislocations in the form of low-angle grain boundaries leads to the formation of smaller diffraction domains and decreased crystallite size [22,26].

Figure 6 shows the SEM images of the AlCrCuFeNi HEA powder samples after different milling times. As illustrated in Figure 6a,b, at the early stages of the MA, the powder particles have plate-like morphology. In this stage, the metal powder samples are still soft and ductile; therefore, particles easily deform into long lamellae with the impact of the balls and the brittle ones crumble into finer particles. The particle size measurements revealed that average particle size of the 10-h-milled sample varied within the wide range of 1–35 μm, but for the 30-h-milled sample this range decreased to 2–27 μm. Deformation,

fracture, and cold welding are the main mechanisms governing particle size during the MA process [14,18]. In the primary stage of MA (low milling time), particles are ductile and can withstand deformation without fracture. Therefore, a larger number of plate-like particles alongside the primary powder particles widen the size range. With increase in milling time, fracturing of plate-like particles due to work hardening and cold welding leads to the narrowing of the size range of particles; the average diameter of particles after 50 h of milling is within the range of 4–29 μm. At higher milling times, a balance is reached between fracture and cold welding that changes the morphology of particles to spherical shape and reduces the particle size rage to 5–24 μm.

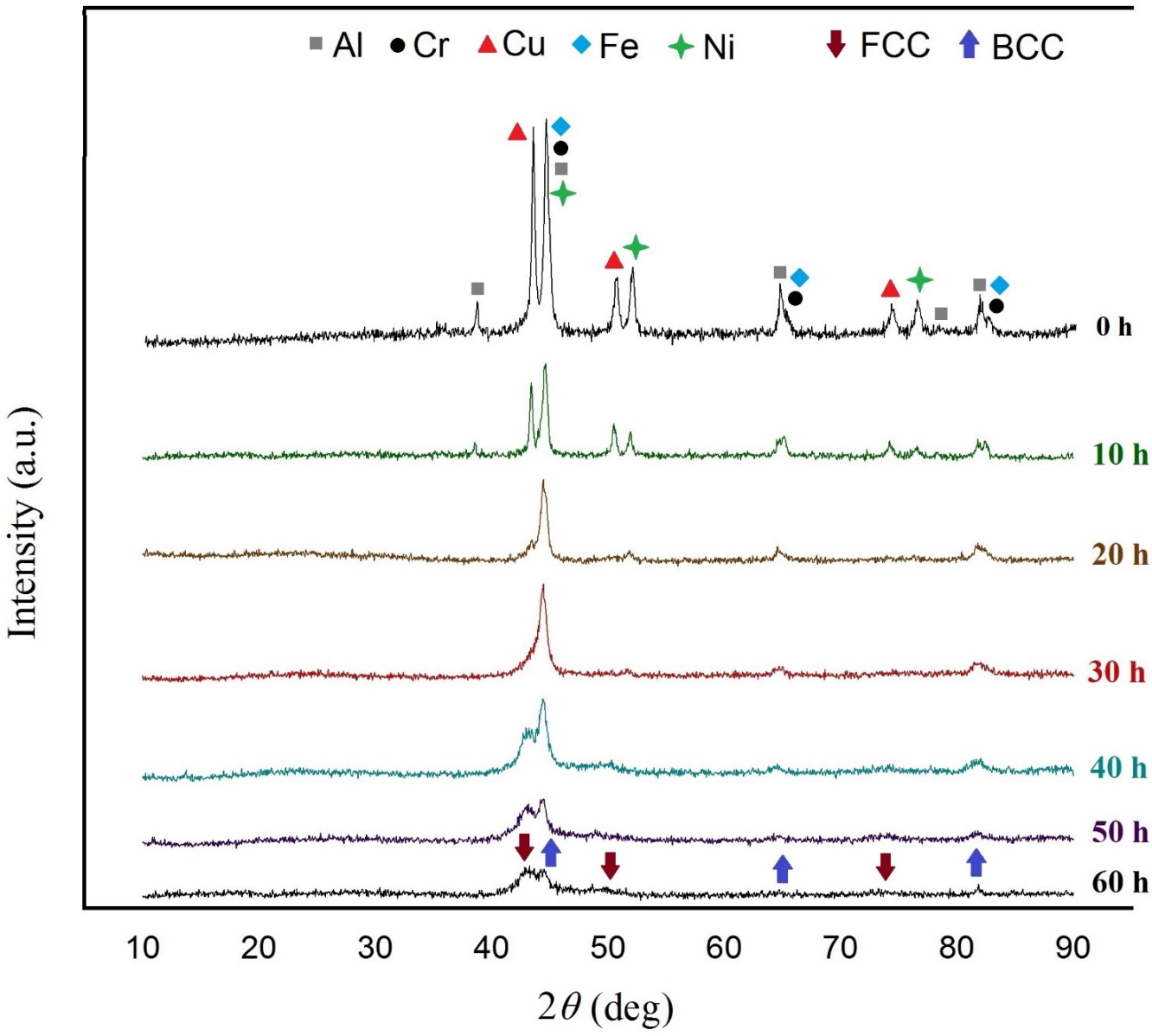

Figure 4. XRD patterns of the AlCrCuFeNi HEA after different time periods of mechanical alloying.

Figure 7 shows the EDS-point analysis of the 60-h-milled powder samples. The atomic percentage and chemical composition of the elements in this sample are close to that of the initial powder. A slight separation of Fe and Cr from the balls and vial might be the cause of the minor increase in their weight percent. Moreover, the presence of oxygen is attributed to the partial oxidation of the powder particles; however, due to the low amount of oxidation, no oxide phase was detected in the XRD test (Figure 1). The sources of

oxygen during MA can be the decomposition of the stearic acid and imperfectly protected atmosphere, before the process and/or after the process, during the tests. The oxygen entered into the system reacts with the surface of the particle powders, especially Al, which can easily react with oxygen.

3.4. Thermal Behavior of the Alloy

Thermal stability of the AlCrCuFeNi alloy was analyzed using DSC analysis and different annealing heat treatments. Figure 8 illustrates the DSC curve for the 60-h-milled AlCrCuFeNi HEA (with 2 wt. % of PCA) heated from room temperature to 1200 °C at a heating rate of 10 °C/min. In the DSC curves, one endothermic peak at 72 °C and two exothermic peaks at 572 and 706 °C can be seen. The first endothermic peak at about 72 °C can be related to the energy absorption of the residual PCA evaporation. The long exothermic line from 100 to 520 °C indicates the release of internal stresses introduced by lattice strain and structural deformation [30], and the two exothermic peaks may be related to the energy released during phase transformations.

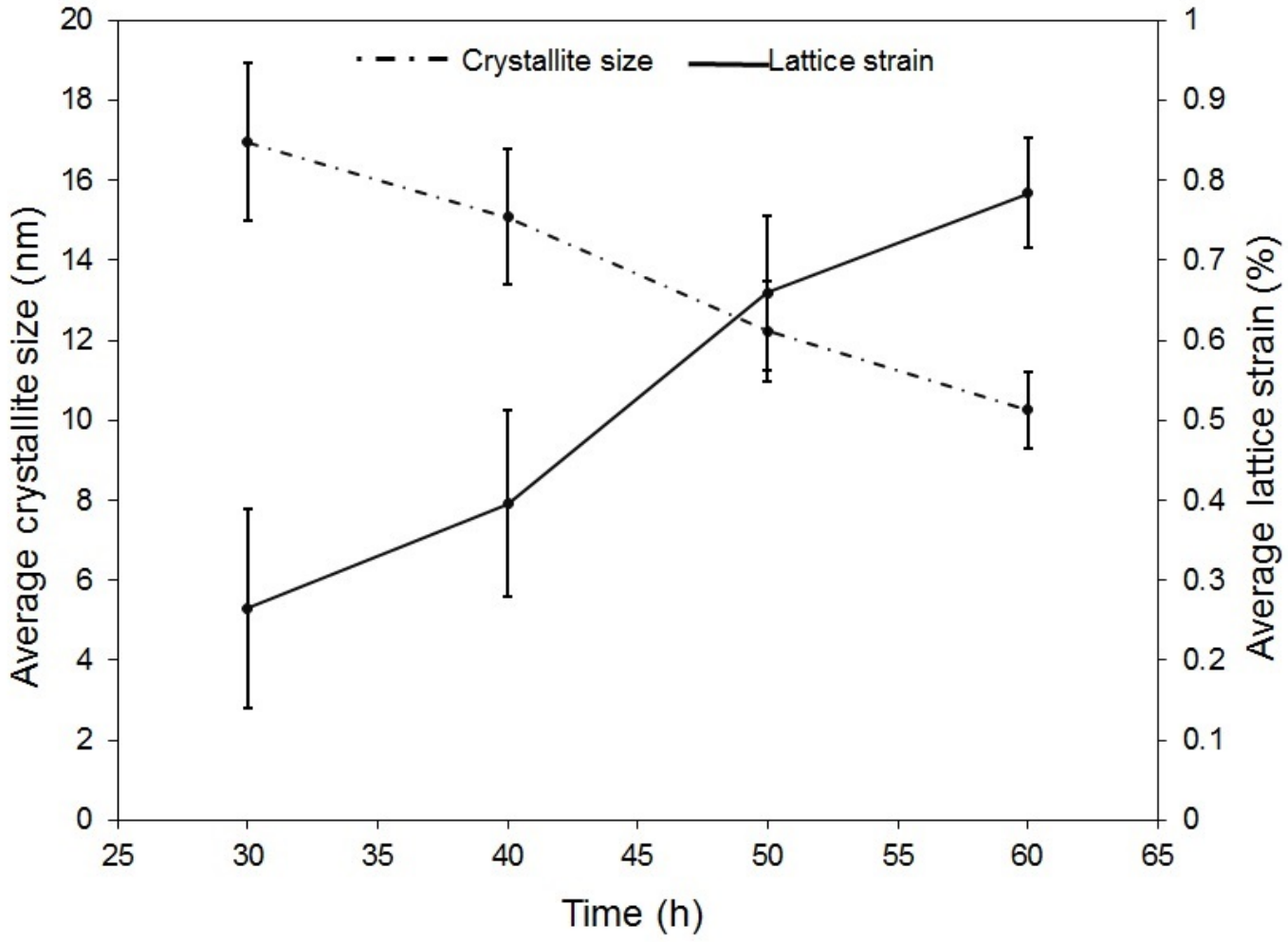

Figure 5. Average crystallite size (nm) and lattice strain (%) of AlCrCuFeNi HEA as a function of milling time.

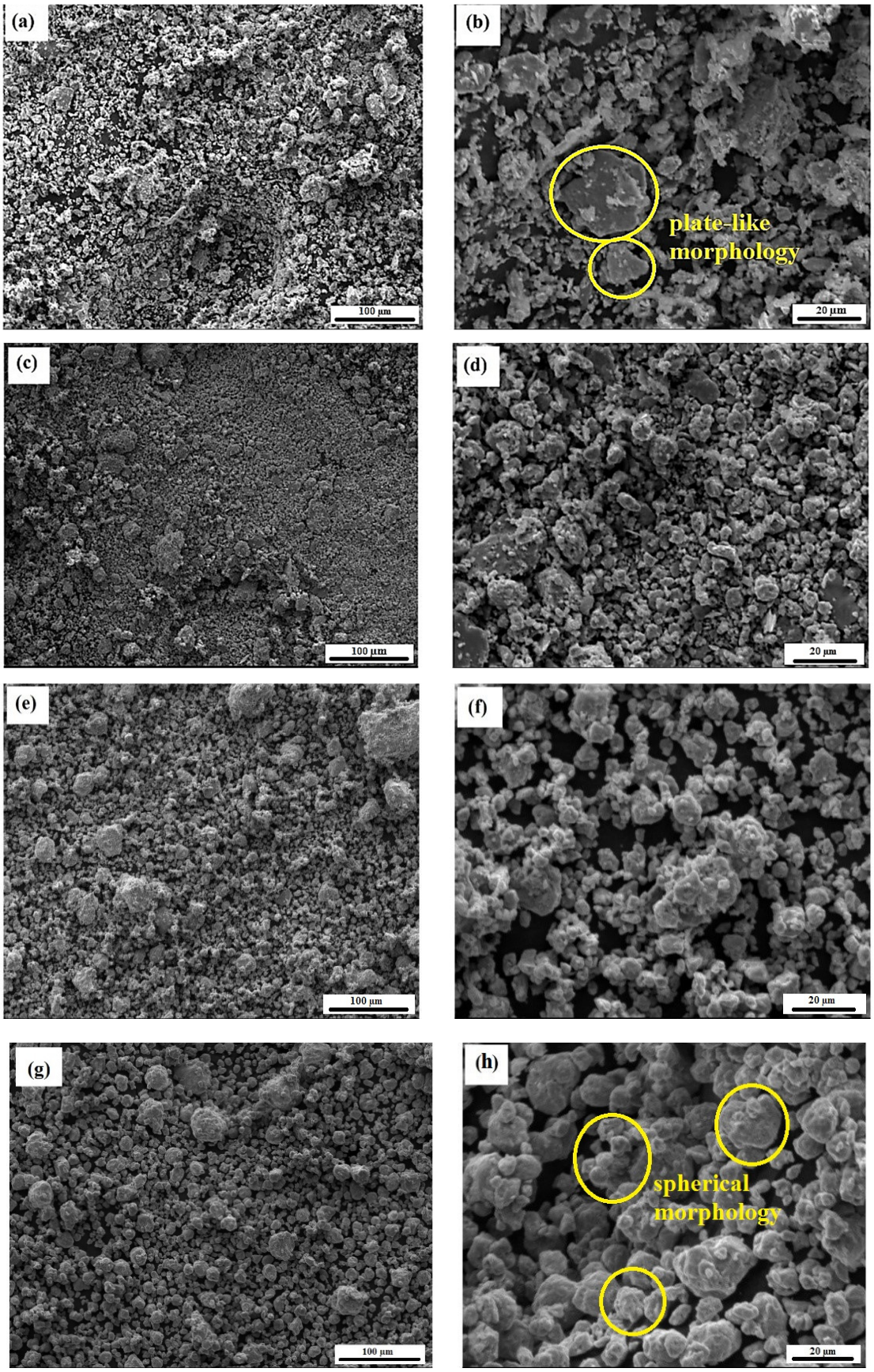

Figure 6. SEM images of the AlCrCuFeNi HEA after (**a**,**b**) 10 h, (**c**,**d**) 30 h, (**e**,**f**) 50 h, and (**g**,**h**) 60 h of milling.

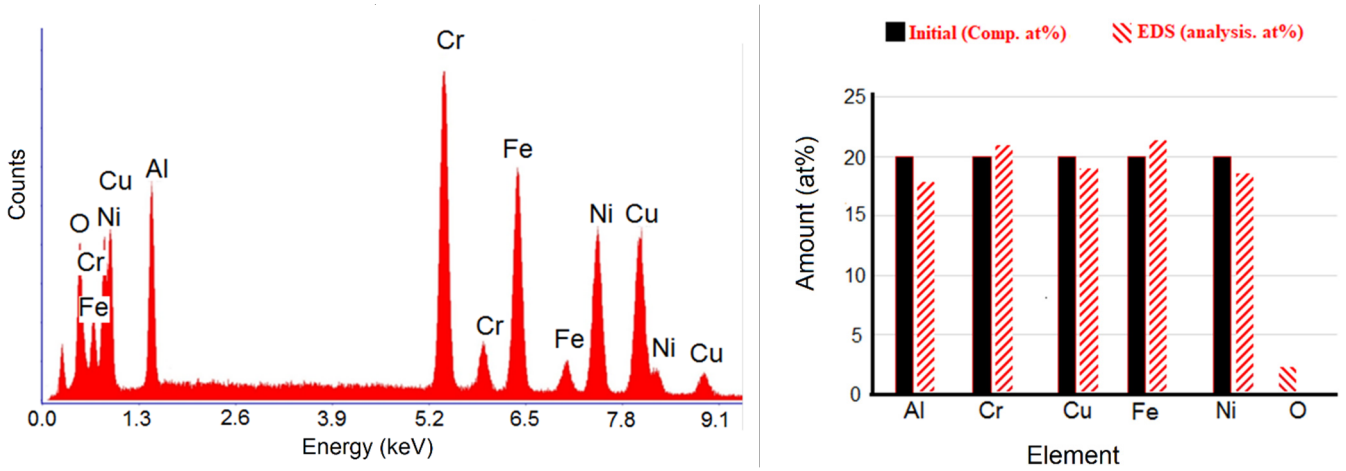

Figure 7. The EDS spectrum (**a**) and quantitative analysis (**b**) of AlCrCuFeNi alloy after 60 h of milling.

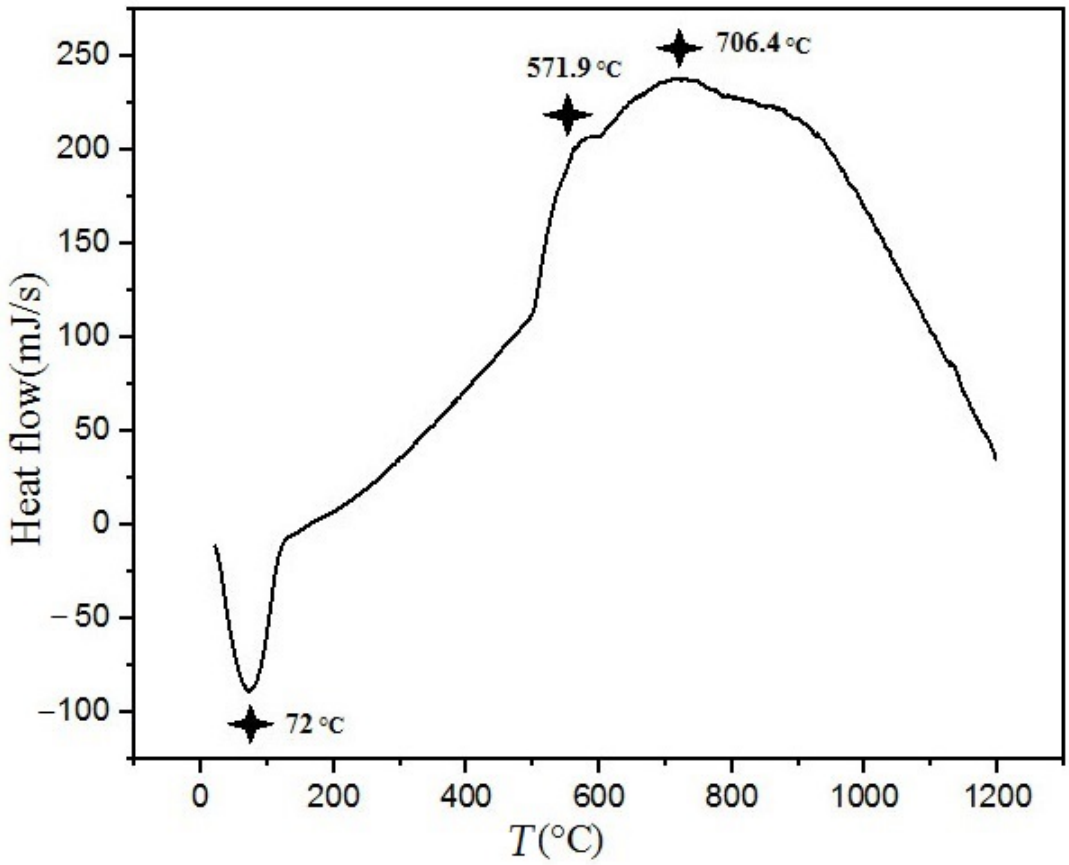

Figure 8. Differential Scanning Calorimetry (DSC) curve of AlCrCuFeNi HEA.

To identify the phase transformations during heating of the alloy, which can be associated with each peak in the DSC curve, 60-h-as-milled powder samples were annealed at different temperatures (from 400 to 1000 °C) for 1 h at a heating rate of 10 °C/min. Figure 9 presents the XRD patterns of the heat-treated alloy at different temperatures. MA is known as a non-equilibrium process and, during heat treatment, the fraction of metastable supersaturated solid solution phases might change, and new stable phases may form in the structure [30]. As revealed in Figure 9, after heat treatment at 400 °C, the XRD

pattern of the annealed powder is similar to that of the powder milled for 60 h and it consists of an FCC and a BCC phase, which is in accordance with the DSC results. By increasing annealing temperature to 600 °C, a sigma phase (σ), which is an intermediate phase with a chemical composition of Fe-Cr, formed in the alloy. This σ phase has a body-centered tetragonal structure and precipitates between 600 and 1000 °C [35]. Additionally, at 600 °C, the conversion of the BCC solid solution phase to an ordered B2 solid solution (β1-ordered B2) took place, and the formation of a peak at the diffraction angle of $2\theta = 31.12°$ revealed this phenomenon. The ordered B2 solid solution mainly consists of Al-Ni in which other elements have dissolved and the high negative enthalpy of mixing between these two elements compared to other atomic pairs is the major reason for its formation [2]. With increase in temperature to 800 °C, the FCC phase decomposed into two new FCC phases with different lattice parameters, which are 0.36179 and 0.36095 nm (lattice parameters are close to that of Cu (0.3615 nm)). Yorkova et al. [13] reported that in the AlCrCuFeNi alloy system (synthesized through the MA method with 580 rpm rotation speed) an FCC phase formed during annealing heat treatment and its fraction increased with increase in temperature. This difference in results can be attributed to the significantly higher milling time that leads to the transference of a higher amount of energy to the particles during MA. The higher amount of energy causes a metastable situation and leads to a rapid decomposing of the alloy at high temperature.

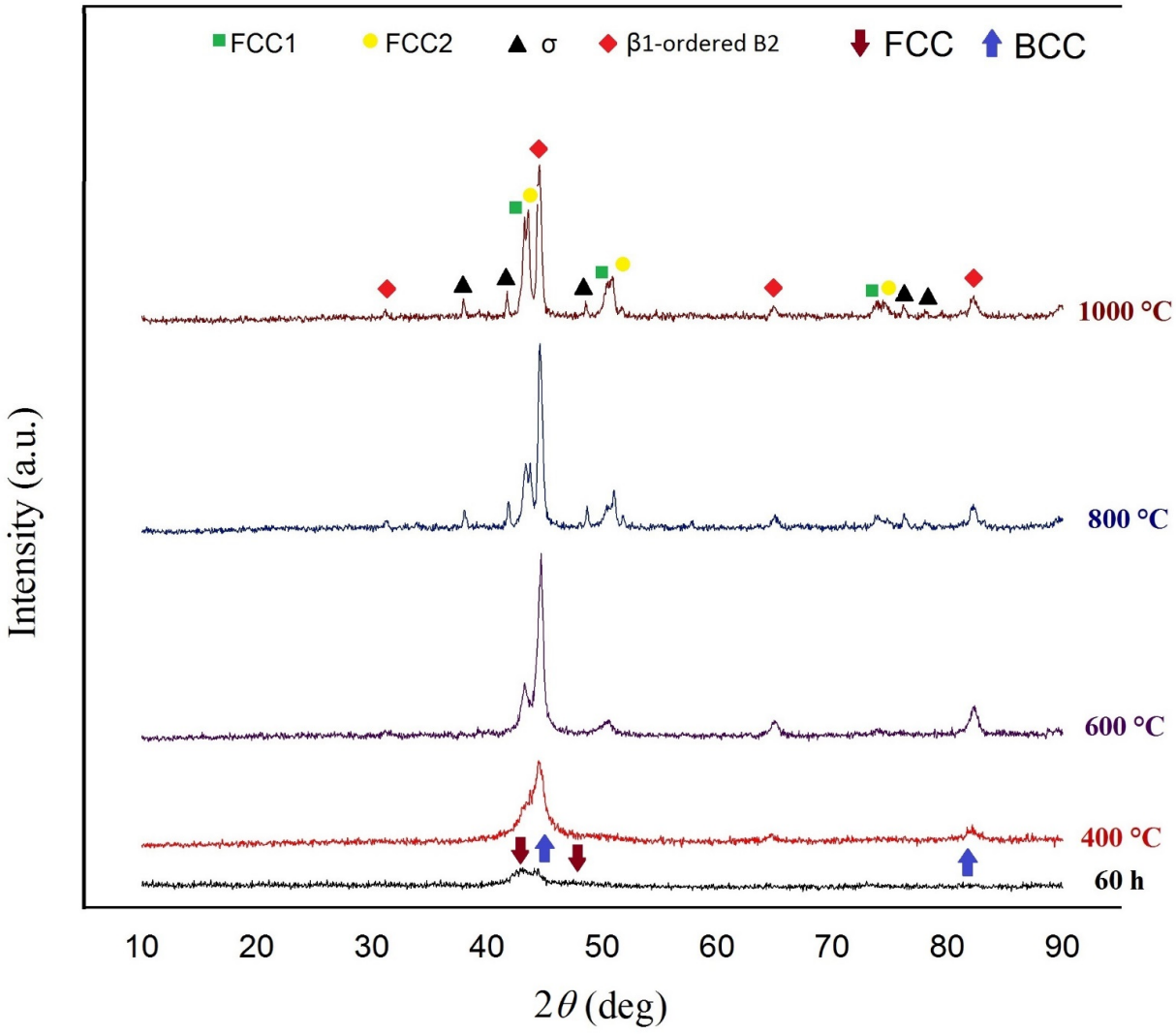

Figure 9. XRD patterns of annealed AlCrCuFeNi HEA powders at different temperatures.

4. Conclusions

In this study, AlCrCuFeNi HEA was successfully synthesized through MA at a milling speed of 350 rpm. Moreover, effects of stearic acid content (PCA), milling time, and annealing heat-treatment on the microstructure and structural properties of the HEA powder were investigated. The following conclusions can be stated:

- Thermodynamic measurements predict the formation of a dual-phase HEA in the AlCrCuFeNi alloying system, which was achieved after 60 h of milling including an FCC and a BCC solid solution phase.
- It was seen that increasing the amount of PCA can postpone the alloying process during MA and lead to a decrease in lattice strain and an increase in crystallite size. The morphology of particles also changed from a spherical shape to a plate-like shape with increase in PCA amount.
- Investigation of milling time revealed that with increase in milling time, lattice strain declines and crystallite size increases, and a 60-h-milling time was needed for achieving the final dual-phase HEA.
- Thermal analysis revealed phase stability up to 400 °C. At 600 °C, a sigma phase (σ), and a B2-ordered solid solution formed in the alloy. In addition, with the increasing of the heat treatment temperature to 800 °C the FCC phase decomposed into two new FCC phases.

Author Contributions: Conceptualization, N.Y. and M.R.T.; methodology, M.R.T.; software, N.Y.; validation, N.Y., M.R.T. and A.S.; formal analysis, N.Y.; investigation, N.Y.; resources, M.R.T.; data curation, N.Y.; writing—original draft preparation, N.Y. and A.S.; writing—review and editing, A.S.; visualization, A.S.; supervision, M.R.T. and P.C.; project administration, M.R.T.; funding acquisition, M.R.T. All authors have read and agreed to the published version of the manuscript.

Funding: This research received no external funding.

Data Availability Statement: Data presented in this article are available at request from the corresponding author.

Conflicts of Interest: The authors declare no conflict of interest.

References

1. Tsai, M.-H.; Yeh, J.-W. High-entropy alloys: A critical review. *Mater. Res. Lett.* **2014**, *2*, 107–123. [CrossRef]
2. Gao, M.C.; Yeh, J.-W.; Liaw, P.K.; Zhang, Y. *High-Entropy Alloys*; Springer International Publishing: Cham, Switzerland, 2016.
3. Shabani, A.; Toroghinejad, M.R. Investigation of microstructure, texture, and mechanical properties of FeCrCuMnNi multiphase high entropy alloy during recrystallization. *Mater. Charact.* **2019**, *154*, 253–263. [CrossRef]
4. Ji, W.; Fu, Z.; Wang, W.; Wang, H.; Zhang, J.; Wang, Y.; Zhang, F. Mechanical alloying synthesis and spark plasma sintering consolidation of CoCrFeNiAl high-entropy alloy. *J. Alloy Compd.* **2014**, *589*, 61–66. [CrossRef]
5. Shabani, A.; Toroghinejad, M.R. Evaluation of microstructure and texture formation during annealing of cold-rolled FeCrCuMnNi multiphase high-entropy alloy. *Trans. Nonferrous Met. Soc. China* **2020**, *30*, 449–462. [CrossRef]
6. Shabani, A.; Toroghinejad, M.R.; Shafyei, A.; Logé, R.E. Microstructure and mechanical properties of a multiphase FeCrCuMnNi high-entropy alloy. *J. Mater. Eng. Perform.* **2019**, *28*, 2388–2398. [CrossRef]
7. Praveen, S.; Murty, B.; Kottada, R.S. Alloying behavior in multi-component AlCoCrCuFe and NiCoCrCuFe high entropy alloys. *Mater. Sci. Eng. A* **2012**, *534*, 83–89. [CrossRef]
8. Kumar, A.; Arora, A.; Chandrakar, R.; Rao, K.R.; Chopkar, M. Nano-crystalline high entropy alloys prepared by mechanical alloying. *Mater. Today Proc.* **2020**, *27*, 1310–1314. [CrossRef]
9. Shivam, V.; Shadangi, Y.; Basu, J.; Mukhopadhyay, N. Evolution of phases, hardness and magnetic properties of AlCoCrFeNi high entropy alloy processed by mechanical alloying. *J. Alloy Compd.* **2020**, *832*, 154826. [CrossRef]
10. Qiao, Y.; Tang, Y.; Li, S.; Ye, Y.; Liu, X.; Bai, S. Preparation of TiZrNbTa refractory high-entropy alloy powder by mechanical alloying with liquid process control agents. *Intermetallics* **2020**, *126*, 106900. [CrossRef]
11. Singh, N.; Shadangi, Y.; Shivam, V.; Mukhopadhyay, N.K. MgAlSiCrFeNi low-density high entropy alloy processed by mechanical alloying and spark plasma sintering: Effect on phase evolution and thermal stability. *J. Alloy Compd.* **2021**, *875*, 159923. [CrossRef]
12. Varalakshmi, S.; Kamaraj, M.; Murty, B. Synthesis and characterization of nanocrystalline AlFeTiCrZnCu high entropy solid solution by mechanical alloying. *J. Alloy Compd.* **2008**, *460*, 253–257. [CrossRef]

13. Yurkova, A.I.; Cherniavsky, V.; Bolbut, V.; Krüger, M.; Bogomol, I. Structure formation and mechanical properties of the high-entropy AlCuNiFeCr alloy prepared by mechanical alloying and spark plasma sintering. *J. Alloy Compd.* **2019**, *786*, 139–148. [CrossRef]
14. Thangaraju, S.; Bouzy, E.; Hazotte, A. Phase stability of a mechanically alloyed CoCrCuFeNi high entropy alloy. *Adv. Eng. Mater.* **2017**, *19*, 1700095. [CrossRef]
15. Tong, C.-J.; Chen, M.-R.; Yeh, J.-W.; Lin, S.-J.; Chen, S.-K.; Shun, T.-T.; Chang, S.-Y. Mechanical performance of the $Al_xCoCrCuFeNi$ high-entropy alloy system with multiprincipal elements. *Metall. Mater. Trans. A* **2005**, *36*, 1263–1271. [CrossRef]
16. Canakci, A.; Varol, T.; Nazik, C. Effects of amount of methanol on characteristics of mechanically alloyed Al–Al2O3 composite powders. *Mater. Technol.* **2012**, *27*, 320–327. [CrossRef]
17. Long, B.; Zuhailawati, H.; Umemoto, M.; Todaka, Y.; Othman, R. Effect of ethanol on the formation and properties of a Cu–NbC composite. *J. Alloy Compd.* **2010**, *503*, 228–232. [CrossRef]
18. Suryanarayana, C. Mechanical alloying and milling. *Prog. Mater. Sci.* **2001**, *46*, 1–184. [CrossRef]
19. Maurice, D.; Courtney, T. Modeling of mechanical alloying: Part I. deformation, coalescence, bdand fragmentation mechanisms. *Metall. Mater. Trans. A* **1994**, *25*, 147–158. [CrossRef]
20. Shaw, L.; Villegas, J.; Luo, H.; Zawrah, M.; Miracle, D. Effects of process-control agents on mechanical alloying of nanostructured aluminum alloys. *Metall. Mater. Trans. A* **2003**, *34*, 159–170. [CrossRef]
21. Nouri, A.; Hodgson, P.; Wen, C. Effect of process control agent on the porous structure and mechanical properties of a biomedical Ti–Sn–Nb alloy produced by powder metallurgy. *Acta Biomater.* **2010**, *6*, 1630–1639. [CrossRef]
22. Duan, Y.; Pang, H.; Wen, X.; Zhang, X.; Wang, T. Microwave absorption performance of $FeCoNiAlCr_{0.9}$ alloy powders by adjusting the amount of process control agent. *J. Mater. Sci. Technol.* **2021**, *77*, 209–216. [CrossRef]
23. Lu, L.; Zhang, Y. Influence of process control agent on interdiffusion between Al and Mg during mechanical alloying. *J. Alloy Compd.* **1999**, *290*, 279–283. [CrossRef]
24. Shabani, A.; Toroghinejad, M.R.; Shafyei, A.; Logé, R.E. Evaluation of the mechanical properties of the heat treated FeCrCuMnNi high entropy alloy. *Mater. Chem. Phys.* **2019**, *221*, 68–77. [CrossRef]
25. Shabani, A.; Toroghinejad, M.R.; Aminaei, M. Effect of prior cold deformation on recrystallization behavior of a multi-phase FeCrCuMnNi high entropy alloy. *Mater. Chem. Phys.* **2021**, *272*, 124991. [CrossRef]
26. Koundinya, N.; Babu, C.S.; Sivaprasad, K.; Susila, P.; Babu, N.K.; Baburao, J. Phase evolution and thermal analysis of nanocrystalline AlCrCuFeNiZn high entropy alloy produced by mechanical alloying. *J. Mater. Eng. Perform.* **2013**, *22*, 3077–3084. [CrossRef]
27. Guo, S. Phase selection rules for cast high entropy alloys: An overview. *Mater. Sci. Technol.* **2015**, *31*, 1223–1230. [CrossRef]
28. Tan, X.-R.; Zhang, G.-P.; Zhi, Q.; Liu, Z.-X. Effects of milling on the microstructure and hardness of $Al_2NbTi_3V_2Zr$ high-entropy alloy. *Mater. Des.* **2016**, *109*, 27–36. [CrossRef]
29. Murali, M.; Kumaresh Babu, S.; Majhi, J.; Vallimanalan, A.; Mahendran, R. Processing and characterisation of nano crystalline $AlCoCrCuFeTi_x$ high-entropy alloy. *Powder Metall.* **2018**, *61*, 139–148. [CrossRef]
30. Zhang, K.; Fu, Z.; Zhang, J.; Shi, J.; Wang, W.; Wang, H.; Wang, Y.; Zhang, Q. Nanocrystalline CoCrFeNiCuAl high-entropy solid solution synthesized by mechanical alloying. *J. Alloy Compd.* **2009**, *485*, L31–L34. [CrossRef]
31. Shabani, A.; Toroghinejad, M.R.; Shafyei, A.; Cavaliere, P. Effect of cold-rolling on microstructure, texture and mechanical properties of an equiatomic FeCrCuMnNi high entropy alloy. *Materialia* **2018**, *1*, 175–184. [CrossRef]
32. Kittel, C.; McEuen, P.; McEuen, P. *Introduction to Solid State Physics*; Wiley: New York, NY, USA, 1996; Volume 8.
33. Sadeghi, B.; Cavaliere, P. Progress of Flake Powder Metallurgy Research. *Metals* **2021**, *11*, 931. [CrossRef]
34. Deng, H.; Xie, Z.; Wang, M.; Chen, Y.; Liu, R.; Yang, J.; Zhang, T.; Wang, X.; Fang, Q.; Liu, C. A nanocrystalline AlCoCuNi medium-entropy alloy with high thermal stability via entropy and boundary engineering. *Mater. Sci. Eng. A* **2020**, *774*, 138925. [CrossRef]
35. Qin, G.; Chen, R.; Mao, H.; Yan, Y.; Li, X.; Schönecker, S.; Vitos, L.; Li, X. Experimental and theoretical investigations on the phase stability and mechanical properties of $Cr_7Mn_{25}Co_9Ni_{23}Cu_{36}$ high-entropy alloy. *Acta Mater.* **2021**, *208*, 116763. [CrossRef]